

Substituted pyrazolo[3,4-*b*]pyridines as human A₁ adenosine antagonists: Developments in understanding the receptor stereoselectivity†

Tiziano Tuccinardi,^a Alessandra Tania Zizzari,^c Chiara Brullo,^b Simona Daniele,^d Francesca Musumeci,^b Silvia Schenone,^{*b} Maria Letizia Trincavelli,^d Claudia Martini,^d Adriano Martinelli,^a Gianluca Giorgi^c and Maurizio Botta^c

Received 7th December 2010, Accepted 9th February 2011

DOI: 10.1039/c0ob01064b

A₁ adenosine receptor antagonists have been proposed to possess an interesting range of potential therapeutic applications. We have already reported the synthesis and the biological characterization of a family of pyrazolo[3,4-*b*]pyridine derivatives as A₁ adenosine ligands endowed with an antagonistic profile. In the present work, we report the LC separation of enantiomers of our most active A₁ antagonists together with the determination of their absolute configuration by means of X-ray crystal structure analysis. Biological assays confirmed a different activity for the two enantiomers, with the *R* one showing the higher human A₁AR affinity. We also developed a homology model of this receptor subtype in order to suggest a binding disposition of the ligands into the hA₁AR. All of the obtained data suggest that the compound's chirality plays a key role in A₁ affinity.

Introduction

The interaction of a drug with its biological target is extremely specific because it depends on the three-dimensional disposition of groups able to determine this specificity. During the development of a drug, it is useful to consider the advantages in terms of action specificity and safety of using homochiral compounds; furthermore chirality could represent a precious source to study a drug's mechanism of action in biological systems.

Adenosine is an endogenous neuromodulator distributed in a wide variety of tissues, in both the periphery and the central nervous system.^{1,2} The effects elicited by adenosine are mediated by its interactions with four receptor subtypes named A₁, A_{2A}, A_{2B}, A₃. These receptors belong to the superfamily of G protein-coupled receptors. The stimulation of adenosine receptors (AR) regulates several effector systems, such as the enzyme adenylyl cyclase. Activation of A₁ and A₃AR leads to an inhibition of

adenylyl cyclase activity, while activation of A_{2A} and A_{2B}AR causes a stimulation of adenylyl cyclase.³ The physiological significance and functions of adenosine have been extensively studied and there has also been research to improve the understanding of ligand-A₁ receptor interactions. In the last two decades, a large number of selective A₁AR ligands have been developed, both xanthine-derivatives and different compounds, usually represented by bi- or tricyclic fused heterocyclic compounds, including purines, deazapurines, pyrazolopyridines, imidazotriazines, thienopyridazines, naphthyridines, quinoxalines, pyridopyrimidines, pyrazoloquinolines and pyrimidoindoles. Also, some examples of monocyclic A₁ antagonists have been reported, including thiazoles, thiadiazoles and pyrimidines.⁴ Different therapeutic applications have been identified in preclinical and clinical studies for A₁AR antagonists, which are effective as potassium-sparing diuretic agents with kidney-protecting properties.⁵ This type of compound is also being tested in the treatment of bradyarrhythmias associated with inferior myocardial infarction, cardiac arrest and cardiac transplant rejection, and could be useful in the treatment of chronic heart diseases.⁶ A₁AR antagonists may also offer a therapeutic opportunity for chronic lung diseases such as asthma, chronic obstructive pulmonary disease and pulmonary fibrosis.⁷ The observation of the effects of caffeine, a classical non-selective adenosine antagonist, on the CNS, such as improvement of awareness and learning, encouraged the search of selective antagonists endowed with central activity. Selective A₁AR antagonists induce cognition enhancement, leading to a general improvement in memory performance, and these actions are potentially useful in the treatment of dementia and anxiety disorders.⁸ Moreover, Trevitt and colleagues recently reported that treatment with the A₁AR antagonist CPT (8-cyclopentyl-1,3-dimethylxanthine)

^aDipartimento di Scienze Farmaceutiche, Università di Pisa, Via Bonanno 6, 56126, Pisa, Italy

^bDipartimento di Scienze Farmaceutiche, Università degli Studi di Genova Viale Benedetto XV 3, 16132, Genova, Italy. E-mail: schensil@unige.it; Fax: (+ 39) 010-353-8358

^cDipartimento Farmaco Chimico Tecnologico, Università degli Studi di Siena, Via De Gasperi 2, 53100, Siena, Italy

^dDipartimento di Psichiatria, Neurobiologia, Farmacologia e Biotecnologie Università degli Studi di Pisa Via Bonanno 6, 56126, Pisa, Italy

^eDipartimento di Chimica, Università degli Studi di Siena, Via De Gasperi 2, 53100, Siena, Italy

† Electronic supplementary information (ESI) available: CD spectra of the enantiomers of compounds 2–5, Ramachandran plot of the starting and energy minimized average structure of the human A₁AR model. CCDC reference number 763003. For ESI and crystallographic data in CIF or other electronic format see DOI: 10.1039/c0ob01064b

in a model of Parkinson's disease produced a dose dependent improvement in locomotion, suggesting that, although the role of A₁AR in Parkinson's disease is still unclear, the A₁AR antagonism may produce therapeutic effects, particularly at the beginning of treatment.⁹

Recently, we synthesized and tested a family of pyrazolo[3,4-*b*]pyridine derivatives as A₁AR ligands.^{10,11} These compounds have shown to be potent and selective antagonists for the bovine A₁ adenosine receptors; furthermore, some of them also showed a promising human A₁ affinity. Extensive computational work has also been carried out showing a good correlation with the available experimental data. In addition, one racemic compound was separated into the two enantiomers, and the biological affinity showed an interesting behaviour with an enantiomeric selectivity that encouraged further analysis of this aspect. These preliminary results prompted us to search for a direct method of enantiomeric separation in order to evaluate the activity of other enantiomerically pure compounds. For this purpose, four high human A₁AR affinity compounds (**1**, **3**, **4**, **5**) and one (**2**) characterized by a poor affinity have been chosen. Direct LC separation into enantiomers, together with the determination of their absolute configuration, is reported. Finally, molecular modelling studies have been carried out with the aim of investigating the interactions of the compounds into the human A₁ receptor model herein developed.

Results and discussion

Enantiomeric separation, specific rotation and circular dichroism (CD) spectra

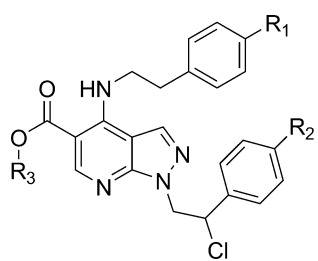
Previously described racemic bovine A₁AR antagonists **2–5** have been resynthesized, as previously described by us.¹¹ The enantiomeric resolution of compounds **2–5** was achieved by using a Chiralcel HPLC OD column and an isocratic elution. Afterwards, a Chiralpak AS column was used for semipreparative purposes, by means of a rapid and practical isocratic method. The collected fractions were then concentrated by rotary evaporation to provide a sizeable amount of each enantiomer. Analytical HPLC re-runs of the elutes were done indicating an enantiomeric purity higher than 95% for each enantiomer. Specific rotation for all the enantiomers was measured and reported in Table 1.

CD spectra of the compounds were measured in ethanol. After subtraction of the solvent baseline, they resulted in mirror images of each other, indicating their enantiomeric nature (see ESI†).

Assignment of absolute configuration

We previously deduced the absolute configuration of compound **1** through CD spectra comparison with a structurally related compound already reported in the literature.^{11,12} In the present study, the enantiomerically pure compound (–)-**1** (blue) has been crystallized and, as shown in Fig. 1, its X-ray crystal structure confirmed our previously *R* configuration hypothesis. It is interesting to note the change in sign of the optical rotation of the *R* and *S* isomers of compounds **3** and **4**, compared with those for compounds **1**, **2** and **5**. Even if the absolute configuration of the stereogenic center could be assigned using powerful modern *ab initio* methods,^{13–15} we obtained it through CD spectra comparison of the stereoisomers (see ESI†). The reported

Table 1 Structures, specific rotation, and experimental affinity (*K_i*) on human A₁AR of the analyzed compounds



Cpds	R ₁	R ₂	R ₃	[α] _D ²⁰	<i>K_i</i> (nM) or % inhibition at 10 μM
(<i>R,S</i>)-1	–OCH ₃	H	–CH ₃	/	94 ± 7.0 ^a
(<i>R</i>)-1	–OCH ₃	H	–CH ₃	–3.45	31 ± 3.2 ^a
(<i>S</i>)-1	–OCH ₃	H	–CH ₃	+3.46	435 ± 42 ^a
(<i>R,S</i>)-2	–OCH ₃	–Cl	–CH ₂ CH ₃	/	15%
(<i>R</i>)-2	–OCH ₃	–Cl	–CH ₂ CH ₃	–17.60	410 ± 40
(<i>S</i>)-2	–OCH ₃	–Cl	–CH ₂ CH ₃	+20.80	10%
(<i>R,S</i>)-3	–OCH ₃	H	–CH(CH ₃) ₂	/	18 ± 1.1
(<i>R</i>)-3	–OCH ₃	H	–CH(CH ₃) ₂	+6.80	11.4 ± 0.35
(<i>S</i>)-3	–OCH ₃	H	–CH(CH ₃) ₂	–4.52	51 ± 2.2
(<i>R,S</i>)-4	–OCH ₃	H	–CH ₂ CH ₃	/	27 ± 3.3
(<i>R</i>)-4	–OCH ₃	H	–CH ₂ CH ₃	+14.41	6.1 ± 1.0
(<i>S</i>)-4	–OCH ₃	H	–CH ₂ CH ₃	–10.73	36 ± 3.2
(<i>R,S</i>)-5	–F	H	–CH ₂ CH ₃	/	17 ± 1.0
(<i>R</i>)-5	–F	H	–CH ₂ CH ₃	–17.5	12 ± 1.2
(<i>S</i>)-5	–F	H	–CH ₂ CH ₃	+14.03	50 ± 4.3

^a Ref. 11

assignment is coherent with the biological data that showed for all the *R* enantiomers a common higher hA₁AR affinity with respect to the corresponding *S* compounds.

Biological assays

The enantiomers were tested for their affinity toward human A₁ CHO transfected cells.¹¹ Binding affinities expressed as affinity constant values (*K_i*) or percent inhibition of the radioligand binding, are reported in Table 1. Activities on human A₁AR have also been remeasured for the racemic compounds. As expected, all of the *R* enantiomers showed higher hA₁AR affinity with respect to the corresponding *S* and racemic compounds.

Molecular modelling

The human A₁AR model was generated using the crystal structure of human A_{2A}AR bound to ZM241385 as a template (3EML).¹⁶ The sequence alignment was studied on the four human adenosine receptor subtypes, the bovine rhodopsin (3C9L),¹⁷ human β₂ adrenergic (2RH1)¹⁸ and turkey β₁ adrenergic receptors (2VT4).¹⁹ These last three sequences were added to the analysis since crystal structures of these complexes are deposited in the Protein Data Bank.²⁰ As shown in Fig. 2, the alignment was guided by the highly conserved amino acid residues, including the asparagine residues N1.50, the LA-AD (L2.46, A2.47, A2.49, and D2.50), and D/ERY-V (D/E3.49, R3.50, Y3.51, and V3.54) motif, the highly conserved tryptophane W4.50, the two prolines P4.59 and P6.50, and the NPXXY motif in TM7 (N7.49, P7.50, and Y7.53).²¹

Following the reported alignment, an A₁ receptor model was built and subjected to a simulated annealing protocol by means of

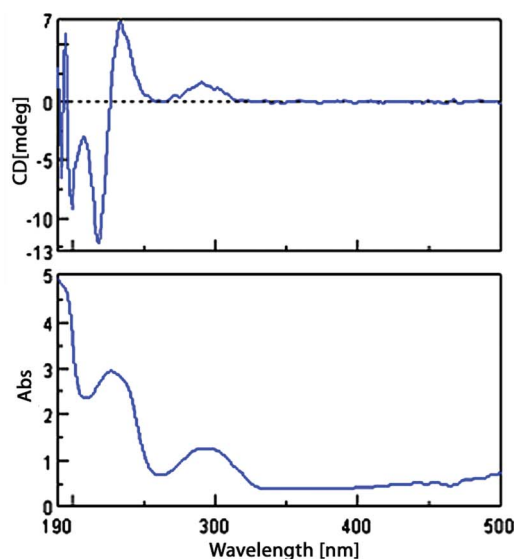


Fig. 1 CD spectra of the enantiomer (–)-**1** and relative X-ray crystal structure. Ortep view of one of the four molecules constituting the asymmetric unit with atom labelling.

the Modeller program.²² The best scoring structure was energy minimized and its backbone conformation was evaluated by PROCHECK²³ (see the Experimental section for details). An analysis of the Psi/Phi Ramachandran plot of the resulting model indicated that only one amino acid of the second extracellular loop had a disallowed geometry (see Fig. S2 in ESI†). The good results obtained from the Psi/Phi Ramachandran plot suggested that the molecular model created of the A_1 receptor could be used for further studies. Compound **4**, which showed the highest A_1 potency, was then docked using the GOLD software²⁴ into the A_1 receptor model. The binding site of the ligand, defined by taking the interaction of ZM241385 in the X-ray structure of A_{2A} AR into account, was individuated in the region between TM2, TM3, and TM5–TM7. The clusterization of the docking results highlighted four different hypothetical ligand dispositions. In order to define the most probable ligand disposition, the four A_1 -ligand complexes were used as starting points for 5 ns of molecular dynamic simulations (MD). We carried out the simulations in

Table 2 MM-PBSA results for the (*R*)-**4**- A_1 AR and (*S*)-**4**- A_1 AR complexes. ΔE_{MM} is the sum of the electrostatic (Ele), van der Waals (VdW) and internal (E_{int}) energy, ΔPB_{Solv} is the sum of the polar (PB) and non-polar (PB_{Sur}) solvation free energy. Finally ΔG_{PBSA} is the sum of the molecular mechanical and solvation free energy. Data are expressed as kcal mol⁻¹

	HYPO1(<i>R</i>)	HYPO2(<i>R</i>)	HYPO3(<i>R</i>)	HYPO4(<i>R</i>)	HYPO3(<i>S</i>)
Ele	-0.85	-5.37	-11.05	-17.19	-6.79
VdW	-60.32	-59.80	-68.28	-55.62	-62.61
E_{int}	0.00	0.00	0.00	0.00	0.00
ΔE_{MM}	-59.48	-65.17	-79.33	-72.81	-69.40
PB_{Sur}	-5.67	-5.80	-5.65	-5.40	-5.90
PB	36.21	37.97	39.42	46.29	37.26
ΔPB_{Solv}	30.54	32.17	28.38	40.88	31.35
ΔG_{PBSA}	-28.94	-32.99	-45.56	-31.93	-38.05

a fully hydrated phospholipid bilayer environment made up of palmitoyleoylphosphatidylcholine (POPC) molecules solvated by TIP3 water molecules, as described in the Experimental section. The system contained 230 POPC molecules, 23 415 water molecules, 12 chlorine ions, the A_1 AR and compound **4**, for a total of 106 121 atoms. The so obtained four MD trajectories were further analyzed through the MM-PBSA method²⁵ that has shown to accurately estimate the ligand–receptor energy interaction.^{26,27} This approach averages the contributions of gas-phase energies, solvation free energies, and solute entropies calculated for snapshots of the complex molecule as well as the unbound components, extracted from MD trajectories, according to the procedure fully described in the Experimental section. As shown in Table 2, the MM-PBSA results strongly suggested that the third ligand disposition hypothesis (HYPO3) is the most reliable, as it showed an interaction energy ($\Delta G_{PBSA} = -45.56$ kcal mol⁻¹) of approximately 12 kcal mol⁻¹ stronger than the other three ligand binding hypotheses.

The stability of the MD simulations was evaluated by calculating the total energy of the systems and analyzing the root-mean-square deviation (RMSD) of all of the α carbons of the TM helices and the heavy atoms from the starting A_1 model structure. Fig. 3 shows the results of this analysis for the (*R*)-**4**- A_1 AR complex (HYPO3). After about 0.5 ns of MD, the system reached an equilibrium, since the total energy for the last 4.5 ns remained approximately constant (Fig. 3, first plot). Analyzing the RMSD of all α carbons of the TM helices from the starting A_1 model structures, we observed that, after 600 ps, it remained between 1.2 and 1.5 Å (Fig. 3, second plot), suggesting that the system was quite stable during the remaining time of MD simulations. This hypothesis was also confirmed by the analysis of the RMSD of all heavy atoms that, after an initial increase, after 600 ps, it remained between 2.6 and 3.2 Å (Fig. 3, second plot). The analysis of the Psi/Phi Ramachandran plot of the energy minimized average structures of the MD's last 4.4 ns indicated that no residue had a disallowed geometry, and only L61, V152 and W156 were in a generously allowed region (Fig. S3 in ESI†). Fig. 4 shows the energy minimized average structures of the last 4.4 ns of the A_1 AR model complexed with compound (*R*)-**4**. The 1*H*-pyrazolo[3,4-*b*]pyridine central scaffold shows a π - π interaction with F171, a lipophilic interaction with V87 and L250, and a hydrogen bond with N254. The ethyl ester chain interacted with T270 and the carbonyl function formed an intramolecular hydrogen bond

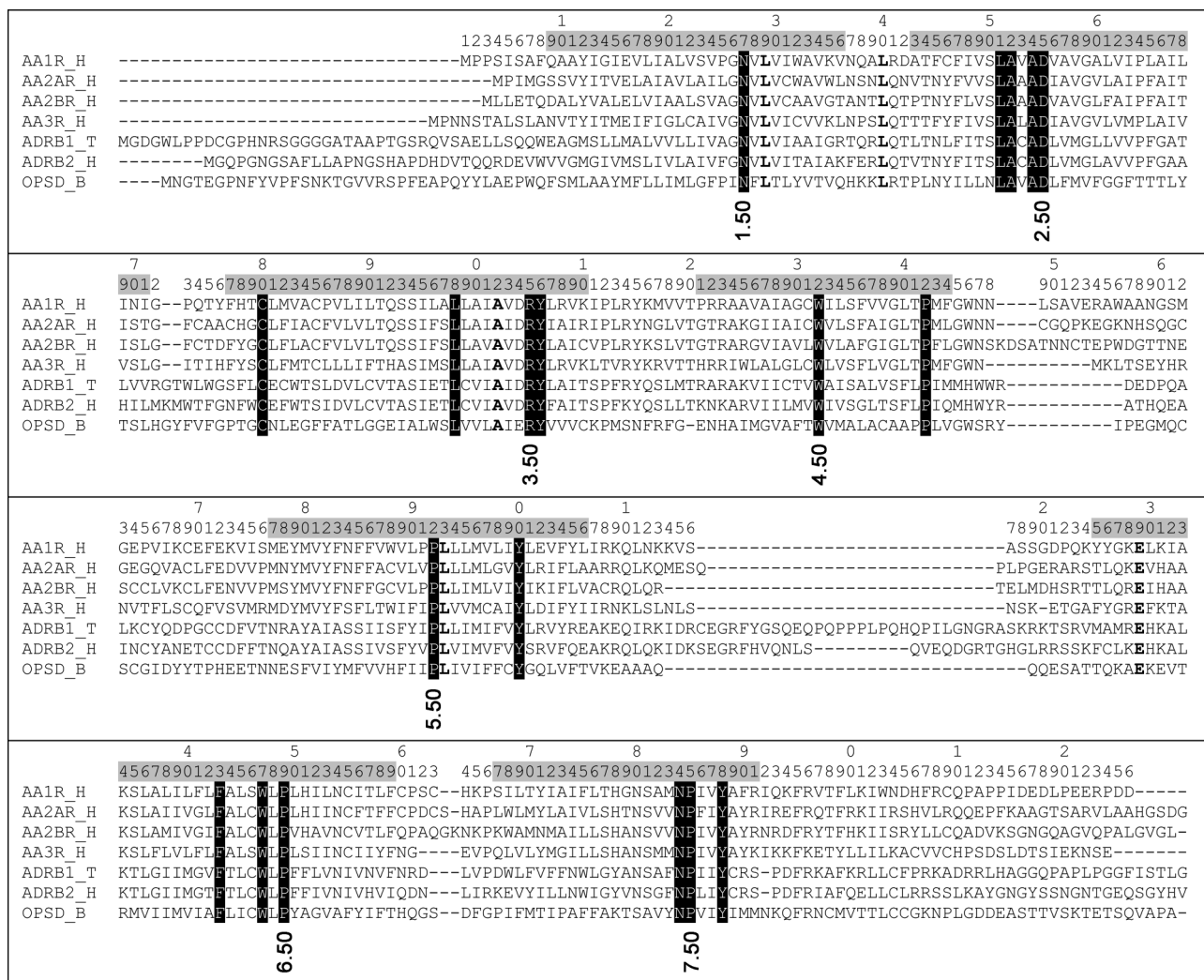


Fig. 2 Alignment of the human adenosine receptors with bovine rhodopsin, human β_2 adrenergic and turkey β_1 adrenergic receptors amino acid sequences. The highly conserved patterns are marked with black background. The other identical residues are in bold characters. In the first and second lines of the alignment scheme are reported the A_1 AR numeration, while the TM domains of A_{2A} AR are reported in gray background.

with the amino group at C4. The 4-methoxyphenethyl substituent interacted with I274 and formed a hydrogen bond with Y251.

Finally the *R*-2-chloro-2-phenethyl substituent interacted with L88, M180 and showed a π - π interaction with H251. The main available experimental data are in agreement with this binding hypothesis; in particular, an important role for F171 and N254 has already been highlighted by the analysis of the X-ray structure of the A_{2A} -ZM241385 complex,¹⁶ furthermore mutagenesis studies have suggested an important role for V87, L88 and H251.²⁸

In order to verify if the receptor model was also able to discriminate between the active *R* and less active *S* enantiomers, the MD simulation procedure applied for the (*R*)-4- A_1 AR complexes was also applied for the *S* enantiomer. As a starting geometry, we used the third docking hypothesis (HYPO3) of (*R*)-4 inverting the chirality of the compound. The analysis of the MD trajectory confirmed the loss of affinity of this compound with respect to the *R* enantiomer. Fig. 4 shows the energy minimized average structures of the last 4.4 ns of the A_1 AR model complexed with compound (*S*)-4; the inversion of the chiral centre determined a shift of the molecule of about 2 Å, and this movement

mainly determined the loss of the hydrogen bonds of the central scaffold with N254 and of the 4-methoxyphenethyl substituent with Y271. Furthermore, the different disposition of the *S*-2-chloro-2-phenethyl substituent also determined the loss of the π - π interaction with H251.

As shown in Table 2, the qualitative analysis is also confirmed by the quantitative one because the analysis of the MM-PBSA results confirmed a greater A_1 AR affinity for the *R* enantiomer, with an energy difference between the interactions of the two enantiomers of about 7 kcal mol⁻¹.

Conclusions

The previously reported racemic mixtures of the selected A_1 AR antagonists were separated into the corresponding enantiomers through a semipreparative HPLC approach. Absolute configuration was determined for (-)-1 enantiomer by means of X-ray crystal structure analysis, then the CD spectra comparison allowed the characterization of the stereochemistry of the other reported compounds. The biological assays confirmed a selective

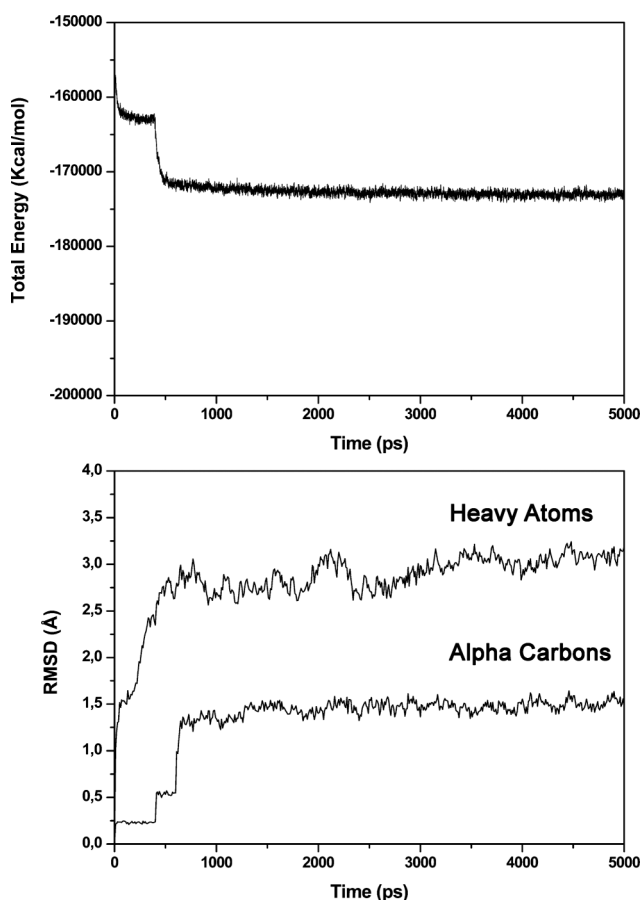


Fig. 3 Analysis of the MD simulation of the (*R*)-4 (HYPO3) complex with A_1AR . In the first plot, the total energy of the system *vs.* the time is reported; the second plot shows the RMSD of the α carbons of the TM helices and the heavy atoms of the receptor from the starting model structure during the simulation.

profile for all of the other enantiomers, with the *R* one showing the highest human A_1AR affinity. In order to suggest a binding disposition of the ligands into the human A_1AR , an homology model of this receptor subtype was developed and, using a mixed

docking/MD simulation approach, a binding disposition for the (*R*)-4 compound was provided. Furthermore, the comparison of the interaction of the (*R*)- and (*S*)-4 enantiomers confirmed the higher affinity of the first one, which was also supported by an MM-PBSA analysis. All of these data suggest that for such high A_1 affinity, the compound's chirality plays a key role that must be taken into consideration in the design of highly potent A_1AR antagonists, and to our knowledge, this is one of the first reports for the A_1 adenosine receptor in this field.^{29,30}

Experimental section

Instrumentation

The chiral separation studies were carried out on a Varian Prostar HPLC system (Varian Analytical Instruments, USA) equipped with a binary pump with a manual injection valve and model Prostar 325 UV-VIS Detector. The CD detection was achieved on a Jasco CD-815 spectropolarimeter circular dichroism detector (Jasco Corporation, Tokyo, Japan). Optical rotations were determined with a Perkin-Elmer Mod 343 polarimeter at 589 nm, using a 10^{-1} dm microcell. Concentrations are expressed as $g mL^{-1}$.

Enantioselective columns and chemicals

The polysaccharide-derived columns were cellulose tris-3,5-dimethylphenylcarbamate (250 mm \times 4.6 mm, Chiralcel OD) and amylose tris 5- α methylbenzyl carbamate (250 mm \times 10 mm, Chiralpak AS), both coated on 10 μm silica gel. All of the above columns were obtained from Daicel (Tokyo, Japan). All of the solvents and reagents were from Sigma Aldrich Srl (Milan, IT).

LC conditions

All separations were carried out at ambient temperature using various mobile phases constituted by n-hexane and 2-propanol mixture. Detection was carried out at 300 nm. The injection volumes were 20 μL and 200 μL for analytical and semipreparative purpose, respectively.

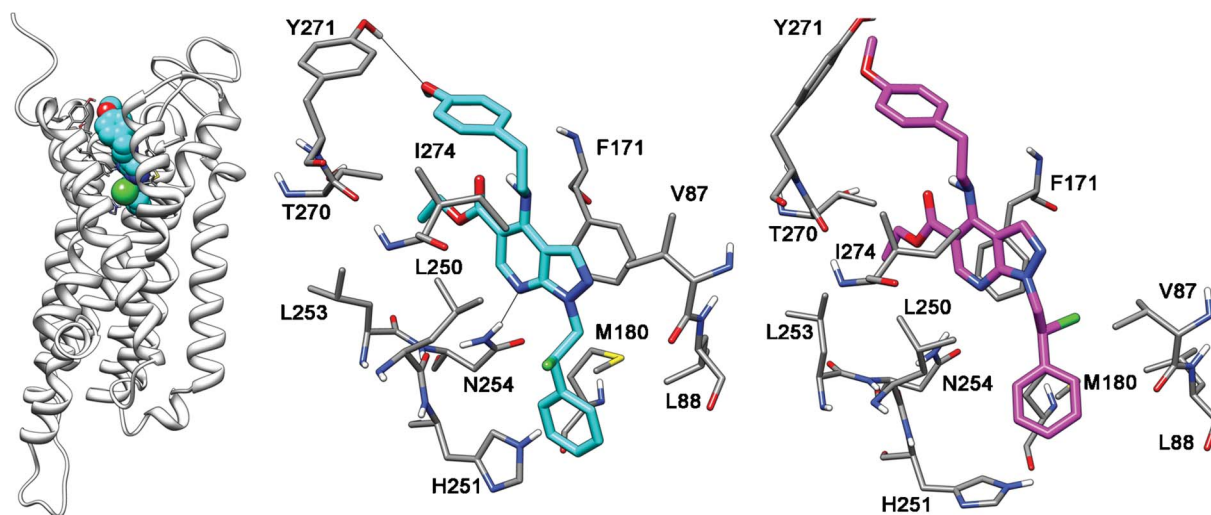


Fig. 4 MD simulation results for the (*R*)-4- A_1AR (light blue) and (*S*)-4- A_1AR (magenta) complex.

Enantioseparation of racemic mixture through a semipreparative method

For semipreparative purposes, Chiralpak AS (250 × 10 mm) was used. The binary solvent system consisted of n-hexane (solvent B) and 2-propanol (solvent A). Samples of racemic mixture were dissolved with the solvents used for mobile phase at the same percentage (v/v). The separation was achieved using the isocratic method. The separation of **2** was achieved using a mobile phase made up of 95% of n-hexane and 5% of 2-propanol at a flow rate of 2.0 mL min⁻¹. The separation of **3** was achieved using 90% of n-hexane and 10% of 2-propanol at a flow rate of 2.0 mL min⁻¹, while the separations of **4** and **5** were achieved using mobile phase made of 85% of n-hexane and 15% of 2-propanol at a flow rate of 2.0 and 3.0 mL min⁻¹, respectively. Analytical re-runs of each eluate were done on Chiralcel OD column with a mobile phase made up of 95% of n-hexane and 5% of 2-propanol at a flow rate of 1.0 mL min⁻¹ for compounds **2**, **4**, **5** and 0.8 mL min⁻¹ for compound **3**. Isolation of single enantiomers of compound **1** has been already reported.¹¹

CD conditions

CD spectra were acquired on a Jasco J-815 dichroism spectrometer with linear data array, two accumulations and with scanning speed of 100 nm min⁻¹. A 1.0 mm path-length quartz cell was used and CD spectra were recorded at room temperature. CD spectra obtained from compounds eluted from the racemic mixture separation were acquired in the 190–500 nm range. Pure enantiomers were dissolved in ethanol to obtain 0.001 mol L⁻¹ solutions. Three scans were averaged and blank-subtracted to obtain the CD spectrum.

Crystallization conditions

Crystals of **1-(B)** suitable for single-crystal X-ray diffraction structure analysis were obtained by slow evaporation of a solution of **1-(B)** in n-hexane/2-propanol, 70 : 30 (v/v) at room temperature (23 °C).

X-ray crystal structure determination

A single crystal of **1-(B)** was submitted to X-ray data collections with a Bruker–Nonius FR591 rotating anode diffractometer with graphite monochromated Mo-K α radiation ($\lambda = 0.71073$ Å) at 120(2)K. The structure was solved by direct methods implemented in the SHELXS-97 program³¹ and the refinement was carried out by full-matrix anisotropic least-squares on F^2 for all reflections for non-H atoms, by using the SHELXL-97 program. The compound crystallizes in the Monoclinic crystal system, $P2_1$ space group, in agreement with its chiral nature. The absolute configuration at C(11) has been determined by the Flack method³² and it resulted to be *R*. CCDC-763003 contains the supplementary crystallographic data. These data can be obtained free of charge from the Cambridge Crystallographic Data Centre via www.ccdc.cam.ac.uk/data_request/cif.

Human A₁AR binding assay

The analyzed compounds were evaluated for their affinity toward human A₁AR stably expressed in CHO cells (kindly

supplied by K.-N. Klotz, Würzburg University, Germany).³³ All compounds were routinely dissolved in dimethyl sulfoxide (DMSO) and diluted in an assay buffer so that the DMSO never exceeded 2%. The compounds were first of all screened at 100 nM and 10 μ M concentration. For the compounds that did not display a significant percentage of binding inhibition (at 10 μ M concentrations), K_i values were not determined. For the active compounds, a dose-response curve using at least six different compound concentrations was performed and the IC₅₀ value determined. IC₅₀ values, computer-generated using a nonlinear regression formula on a computer program (GraphPad, San Diego, CA), were converted to K_i values, knowing the K_d values of radioligand and using the Cheng and Prusoff equation.³⁴

Homology modelling

The crystal structure of human A_{2A}AR bound to ZM241385 was taken from the Protein Data Bank,²⁰ while all the primary sequences were obtained from the SWISS-PROT protein sequence database.³⁵ The sequential alignment was performed by means of CLUSTAL W,³⁶ using the Blosum series as a matrix, with a gap open penalty of 10 and a gap extension penalty of 0.05. The human A₁ and A_{2A}AR show about 45% of identical residues with a CLUSTAL W alignment score of 48. The human A₁ was constructed directly from the coordinates of the corresponding amino acids in A_{2A}AR by means of the Modeller program.²² Starting from this receptor, 10 structures were generated by means of the “very slow MD annealing” refinement method, as implemented in Modeller, and on the basis of the DOPE (discrete optimized protein energy) assess method, the best receptor model was chosen. The backbone conformation of the resulting receptor structure was evaluated by inspection of the Psi/Phi Ramachandran plot obtained from PROCHECK analysis.²³

Docking of (R)-4

The ligand was built using Maestro³⁷ and was subjected to a conformational search (CS) of 1000 steps, using a water environment model (generalized-Born/surface-area model) by means of Macromodel.³⁸ The algorithm used was based on the Monte Carlo method with the MMFFs force field and a distance-dependent dielectric constant of 1.0. The ligand was then energy minimized using the conjugated gradient method until a convergence value of 0.05 kcal/(Å mol) was reached, using the same force field and parameters used for the CS. Automated docking was carried out by means of the GOLD program,²⁴ version 4.1.1. The region of interest used by GOLD was defined in order to contain the residues within 10 Å from the original position of ZM241385 in the A_{2A}AR X-ray structure. The “allow early termination” option was deactivated, while the possibility of clusterizing the results was activated (the RMSD distance clustering was set to 1.5 Å). The remaining GOLD default parameters were used, and the ligand was submitted to 30 genetic algorithm runs by applying the GoldScore fitness function. The clusters showing a GoldScore fitness scoring value that differed less than 10 units with respect to the best docked conformation were taken into account; as a result, four docking conformations were considered.

MD simulations

All simulations were performed using AMBER 10.³⁹ The five complexes (four (*R*)-4-A₁AR and one (*S*)-4-A₁AR systems) were embedded into a phospholipid bilayer made up of POPC molecules. The creation of the phospholipid bilayer and the insertion of the receptor-ligand complexes were carried out using VMD.⁴⁰ MD simulations were carried out using the modified parm94 force field at 300 K. An explicit solvent model of TIP3P water was used. The system was solvated on the “extracellular” and “intracellular” side with a 12 Å water cap. Chlorine ions were added as counterions to neutralize the system. Prior to MD simulations, three steps of energy minimization were carried out. In the first stage, we kept the protein and phospholipids fixed with a position restraint of 100 kcal mol⁻¹ Å⁻² and we just energy minimized the positions of the water molecules. In the second stage, we energy minimized the phospholipid–water system, applying a position restraint of 100 kcal mol⁻¹ Å⁻² on the protein. Finally, we applied a restraint of 30 kcal mol⁻¹ Å⁻² only on the α carbons of the receptor. The three energy minimization stages consisted of 10 000 steps. The first 1000 steps were Steepest Descent, and the last 9000 were Conjugate Gradient. Molecular dynamics trajectories were run using the energy minimized structure as the input, and particle mesh Ewald electrostatics⁴¹ and periodic boundary conditions were used in the simulation. The time step of the simulations was 2.0 fs with a cutoff of 12 Å for the non-bonded interaction. SHAKE was employed to keep all bonds involving hydrogen atoms rigid. A constant-volume was carried out for 200 ps, during which time the temperature was raised from 0 to 300 K (using the Langevin dynamics method). Then, 4800 ps of constant-pressure MD were carried out at 300 K. In the first 400 ps, all of the α carbons of the receptor were blocked with a harmonic force constant. This was decreased during the 400 ps from 10 to 1 kcal mol⁻¹ Å⁻¹. In the last 4400 ps, there were no constraints. The final structure was obtained as the average of the last 4400 ps of MD energy minimized with the CG method until a convergence of 0.05 kcal mol⁻¹ Å⁻¹ was reached. The backbone conformation of the resulting receptor structure was evaluated by inspection of the γ/f Ramachandran plot obtained from PROCHECK analysis.²³ The General Amber Force Field (GAFF) parameters were assigned to POPC molecules. The partial charges were calculated using the AM1-BCC method, as implemented in the Antechamber suite of AMBER 10.

Energy evaluation

We extracted from the last 4400 ps of MD of the ligand–receptor complexes, 88 snapshots (at time intervals of 50 ps) for each species (complex, receptor and ligand). The various MM-PBSA energy terms in equation 1 were computed as follows.

$$G = G_{\text{polar}} + G_{\text{nonpolar}} + E_{\text{mm}} - TS \quad (1)$$

Electrostatic, van der Waals and internal energies (E_{mm}) were obtained using the SANDER module in AMBER 10. Polar energies (G_{polar}) were obtained from the PBSA module of the AMBER 10 program (using the Poisson–Boltzman method) applying dielectric constants of 1 and 80 to represent the gas and water phases, respectively. Nonpolar energies (G_{nonpolar}) were determined using the MOLSURF program. In order to compare

the energetic interactions of the two enantiomers of the same ligand into the receptor, we took only the first three terms of eqn (1) into account, considering the entropic value as approximately constant.

Acknowledgements

National Interest Research Projects (PRIN_2008_5HR5JK) is gratefully acknowledged.

References

- 1 K. A. Jacobson, P. J. van Galen and M. Williams, *J. Med. Chem.*, 1992, **35**, 407–422.
- 2 J. W. Daly, *J. Med. Chem.*, 1982, **25**, 197–207.
- 3 S. A. Poulsen and R. J. Quinn, *Bioorg. Med. Chem.*, 1998, **6**, 619–641.
- 4 S. Schenone, C. Brullo, F. Musumeci, O. Bruno and M. Botta, *Curr. Top. Med. Chem.*, 2010, **10**, 878–901.
- 5 P. S. Modlinger and W. J. Welch, *Curr. Opin. Nephrol. Hypertens.*, 2003, **12**, 497–502.
- 6 R. H. Shah and W. H. Frishman, *Cardiol. Rev.*, 2009, **17**, 125–131.
- 7 C. N. Wilson, A. Nadeem, D. Spina, R. Brown, C. P. Page and S. J. Mustafa, *Handb. Exp. Pharmacol.*, 2009, **193**, 329–362.
- 8 T. Maemoto, M. Tada, T. Mihara, N. Ueyama, H. Matsuoka, K. Harada, T. Yamaji, K. Shirakawa, S. Kuroda, A. Akahane, A. Iwashita, N. Matsuoka and S. Mutoh, *J. Pharmacol. Sci.*, 2004, **96**, 42–52.
- 9 J. Trevitt, C. Vallance, A. Harris and T. Goode, *Pharmacol., Biochem. Behav.*, 2009, **92**, 521–527.
- 10 F. Manetti, S. Schenone, F. Bondavalli, C. Brullo, O. Bruno, A. Ranise, L. Mosti, G. Menozzi, P. Fossa, M. L. Trincavelli, C. Martini, A. Martinelli, C. Tintori and M. Botta, *J. Med. Chem.*, 2005, **48**, 7172–7185.
- 11 T. Tuccinardi, S. Schenone, F. Bondavalli, C. Brullo, O. Bruno, L. Mosti, A. T. Zizzari, C. Tintori, F. Manetti, O. Ciampi, M. L. Trincavelli, C. Martini, A. Martinelli and M. Botta, *ChemMedChem*, 2008, **3**, 898–913.
- 12 F. Da Settimo, G. Primofiore, C. La Motta, S. Taliani, F. Simorini, A. M. Marini, L. Mugnaini, A. Lavecchia, E. Novellino, D. Tuscano and C. Martini, *J. Med. Chem.*, 2005, **48**, 5162–5174.
- 13 R. K. Kondru, P. Wipf and D. N. Beratan, *Science*, 1998, **282**, 2247–2250.
- 14 R. K. Kondru, P. Wipf and D. N. Beratan, *J. Phys. Chem. A*, 1999, **103**, 6603–6611.
- 15 P. L. Polavarapu, *Chirality*, 2002, **14**, 768–781.
- 16 V. P. Jaakola, M. T. Griffith, M. A. Hanson, V. Cherezov, E. Y. Chien, J. R. Lane, A. P. Ijzerman and R. C. Stevens, *Science*, 2008, **322**, 1211–1217.
- 17 R. E. Stenkamp, *Acta Crystallogr., Sect. D: Biol. Crystallogr.*, 2008, **D64**, 902–904.
- 18 V. Cherezov, D. M. Rosenbaum, M. A. Hanson, S. G. Rasmussen, F. S. Thian, T. S. Kobilka, H. J. Choi, P. Kuhn, W. I. Weis, B. K. Kobilka and R. C. Stevens, *Science*, 2007, **318**, 1258–1265.
- 19 T. Warne, M. J. Serrano-Vega, J. G. Baker, R. Moukhametdzianov, P. C. Edwards, R. Henderson, A. G. Leslie, C. G. Tate and G. F. Schertler, *Nature*, 2008, **454**, 486–491.
- 20 H. M. Berman, J. Westbrook, Z. Feng, G. Gilliland, T. N. Bhat, H. Weissig, I. N. Shindyalov and P. E. Bourne, *Nucleic Acids Res.*, 2000, **28**, 235–242.
- 21 A. Martinelli and T. Tuccinardi, *Expert Opin. Drug Discovery*, 2006, **1**, 459–476.
- 22 A. Fiser, R. K. Do and A. Sali, *Protein Sci.*, 2000, **9**, 1753–1773.
- 23 R. A. Laskowski, M. W. MacArthur, D. S. Moss and J. M. Thornton, *J. Appl. Crystallogr.*, 1993, **26**, 283–291.
- 24 M. L. Verdonk, J. C. Cole, M. J. Hartshorn, C. W. Murray and R. D. Taylor, *Proteins: Struct., Funct., Bioinf.*, 2003, **52**, 609–623.
- 25 P. A. Kollman, I. Massova, C. Reyes, B. Kuhn, S. Huo, L. Chong, M. Lee, T. Lee, Y. Duan, W. Wang, O. Donini, P. Cieplak, J. Srivivasan, D. A. Case and T. E. Cheatham, 3rd, *Acc. Chem. Res.*, 2000, **33**, 889–897.
- 26 T. Tuccinardi, S. Bertini, A. Martinelli, F. Minutolo, G. Ortore, G. Placanicca, G. Prota, S. Rapposelli, K. E. Carlson, J. A. Katzenellenbogen and M. Macchia, *J. Med. Chem.*, 2006, **49**, 5001–5012.

-
- 27 T. Tuccinardi, F. Manetti, S. Schenone, A. Martinelli and M. Botta, *J. Chem. Inf. Model.*, 2007, **47**, 644–655.
- 28 A. Martinelli and T. Tuccinardi, *Med. Res. Rev.*, 2008, **28**, 247–277.
- 29 S. A. Poulsen, D. J. Young and R. J. Quinn, *Bioorg. Med. Chem. Lett.*, 2001, **11**, 191–193.
- 30 J. R. Pfister, L. Belardinelli, G. Lee, R. T. Lum, P. Milner, W. C. Stanley, J. Linden, S. P. Baker and G. Schreiner, *J. Med. Chem.*, 1997, **40**, 1773–1778.
- 31 G. M. Sheldrick and T. R. Schneider, *Methods Enzymol.*, 1997, **277**, 319–343.
- 32 H. D. Flack, *Acta Crystallogr., Sect. A: Found. Crystallogr.*, 1983, **A39**, 876–881.
- 33 O. Lenzi, V. Colotta, D. Catarzi, F. Varano, G. Filacchioni, C. Martini, L. Trincavelli, O. Ciampi, K. Varani, F. Marighetti, E. Morizzo and S. Moro, *J. Med. Chem.*, 2006, **49**, 3916–3925.
- 34 Y. Cheng and W. H. Prusoff, *Biochem. Pharmacol.*, 1973, **22**, 3099–3108.
- 35 E. Gasteiger, A. Gattiker, C. Hoogland, I. Ivanyi, R. D. Appel and A. Bairoch, *Nucleic Acids Res.*, 2003, **31**, 3784–3788.
- 36 J. D. Thompson, D. G. Higgins and T. J. Gibson, *Nucleic Acids Res.*, 1994, **22**, 4673–4680.
- 37 *Maestro*, version 9.0, Schrödinger Inc: Portland, OR, 2009.
- 38 *Macromodel*, version 9.7, Schrödinger Inc: Portland, OR, 2009.
- 39 D. A. Case, T. A. Darden, T. E. Cheatham III, C. L. Simmerling, J. Wang, R. E. Duke, R. Luo, M. Crowley, R. C. Walker, W. Zhang, K. M. Merz, B. Wang, S. Hayik, A. Roitberg, G. Seabra, I. Kolossváry, K. F. Wong, F. Paesani, J. Vanicek, X. Wu, S. R. Brozell, T. Steinbrecher, H. Gohlke, L. Yang, C. Tan, J. Mongan, V. Hornak, G. Cui, D. H. Mathews, M. G. Seetin, C. Sagui, V. Babin, and P. A. Kollman, 2008, AMBER 10, University of California: San Francisco, CA, .
- 40 W. Humphrey, A. Dalke and K. Schulten, *J. Mol. Graphics*, 1996, **14**(33–38), 27–38.
- 41 U. Essmann, L. Perera, M. L. Berkowitz, T. Darden, H. Lee and L. G. Pedersen, *J. Chem. Phys.*, 1995, **103**.